

BEHAVIOR OF THE TOTAL ELECTRON CONTENT DURING GEOMAGNETIC STORM 17 MARCH 2015 OVER THE ARCTIC REGION

Comment [APBS1]: It will be better if the author modify the title in this way "A GEOMAGNETIC STORM IN THE ARCTIC REGION ON MARCH 17, 2015: THE TOTAL ELECTRON CONTENT."

Abstract

We describe the ionospheric response to the St. Patrick's Day storm, which was the biggest geomagnetic storm of the 24th solar cycle up until that point. The storm occurred on March 17–18, 2015. TEC measurements were obtained using Global Positioning System (GPS) receivers of the Canadian High Arctic Ionospheric Network (CHAIN) from three stations: Cambridge Bay, Eureka, and Rabbit Lake. Based on the results, we observed that during stormy conditions, TEC was significantly lower on Cambridge Bay than it was on Eureka and Rabbit Lake.

Comment [APBS2]: Revise the abstract. It should include i. objective, results, and dis

Introduction:

The ionospheric reaction to geomagnetic storms has been one of the essential subjects in space climate research for quite a long time (Gonzalez et al., 1994; Richmond et al., 2000). During geomagnetic storms, the improved infusion of energy from the sun oriented breeze causes unsettling influences in the science and elements of the coupled thermosphere and ionosphere framework (Prölss, et al., 1995; Buonsanto, et al., 1999). Many examinations have been given to considering ionospheric storm impacts close to the F district top (Fuller-Rowell et al., 1994; Burns et al., 1995; Mendillo, 2006), yet the ionospheric reaction to geomagnetic storms is as yet not completely comprehended.

Examinations of ionosphere elements and aggravations during geomagnetic storms are still of high significance because of impact of the ionosphere on the space climate. The ionosphere, as a functioning layer, assumes a significant part in the space climate because of its affectability to the sun powered action. Thusly, the space climate influences satellite frameworks, energy transport, air traffic and, in outcome, the economy (Schrijver et al. 2015). Subsequently, the investigations of the ionosphere conduct assume a vital part in comprehension and estimating of the space climate. The ionosphere is a layer of the air comprising for the most part of ionized particles, which causes the satisfy light electromagnetic signs to be deferred, changes in signal strength and other unfriendly impacts. The extent of these ionospheric impacts generally relies upon the condition of the shifting ionosphere, its complete electron content (TEC) and the recurrence of electromagnetic waves. The unique changes of the ionosphere are most effectively separated into normal and abrupt ones. Standard changes are straightforwardly identified with the periodicity of the variables impacting them, like the sun powered cycle. These ordinary varieties are to some degree simple to display (Bilitza et al., 2008; Maruyama et al. 2009). The ionospheric storms (aggravations in the earthly ionosphere delivered by geomagnetic storms) cause huge unsettling influences for innovative frameworks, for example, the static or dynamical situating with GNSS satellites, and others, which rely upon the transionospheric correspondences. Essentially, in correlation with under calm conditions, the electron thickness

can increment or diminishing during geomagnetic storm periods. These changes, which have been called positive ionospheric tempest or positive tempest impact and negative ionospheric tempest or negative tempest impact individually, happen in light of the fact that there is critical energy input (from the sun based breeze) into the polar ionosphere, for the most part over a time of a few hours to a day. A few driver powers have been utilized to clarify the ionospheric impacts during storms at various scopes. For instance, it is accepted that level convection overwhelms in the polar covers, and structure changes, molecule precipitation and electric fields rule in the auroral zones, while electric fields, meridional breezes and creation changes rule at tropical and low scopes. In the auroral and polar ionosphere, those abnormalities at an alternate scale have a typical element during geomagnetic storms, which causes vacillations in the Total Electron Content (TEC). Thusly, the limited scale ionospheric plasma thickness inconsistencies produce quick change in the abundance and period of transionospheric radio signs, which is known as sparkle. The huge scope inconsistencies and related TEC vacillations an muddle stage vagueness goal, increment the quantity of uncorrected cycle slips and misfortunes of sign lock in GNSS. Since there are moderately inadequate outcomes for TEC. The large-scale irregularities and associated TEC fluctuations can complicate phase ambiguity resolution, increase the number of uncorrected cycle slips and losses of signal lock in GNSS. Because there are relatively sparse results for TEC at sub-auroral, auroral and polar latitudes in this paper we analyze the behavior of TEC at three stations located in the Arctic sectors during intense geomagnetic storms in the 2015.

Data and methodology

The GNSS perception information of Crustal Movement Observation Network CHAIN in three stations in particular given in table 1, which incorporates three GPS beneficiaries, are utilized to reproduce the ionospheric complete electron content (TEC) circulation during 17 March, 2015 geomagnetic storm periods. The scope and longitude of these three GPS recipients are displayed in Table 1. Fig. 1 presents the topographical area of GPS beneficiaries over High Latitude stations. The CHAIN GPS recipients are GPS Ionospheric Scintillation and TEC Monitors (GISTMs) model GSV4000B. In outline, a GISTM comprises of a NovAtel OEM4 double recurrence beneficiary with uncommon firmware explicitly arranged to gauge adequacy and stage shine got from the L1 recurrence GPS signals and ionospheric absolute electron content (TEC) got from the L1 and L2 recurrence GPS signals. This collector is fit for following and revealing glimmer and TEC estimations from up to ten GPS satellites in see. Stage and plentifulness information are examined and logged, either in crude structure or detrended, at a pace of 50 Hz. Nine of the ten collectors are as of now took care of by a NovAtel GPS-702 receiving wire, the exemption being the Qikiqtarjuaq recipient what shares an Ashtech ASH701945E_M radio wire with a pre-existing Natural Resources Canada GPS beneficiary through a splitter. At most occasions, 8 to 10 GPS satellites are apparent to a solitary ground recipient. From GPS information we figure the complete electron content (TEC), a worth

coordinated in a 1 m2 section along the satellite to collector ray path. Detective is determined in TEC units (TECu), where 1 TECu = 10^{16} electrons for each square meter.

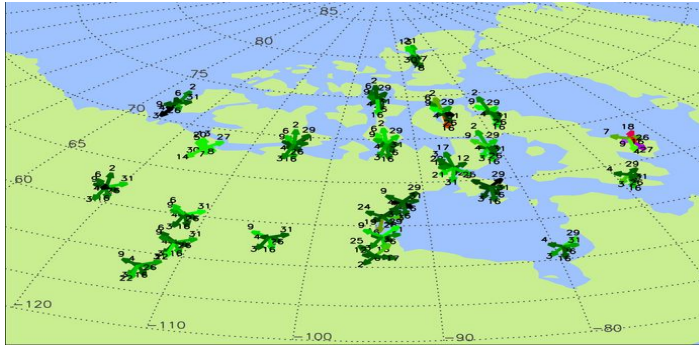


Figure 1: CHAIN Ionspheric Network over Arctic Region

Table 1. Geographic and Geomagnetic Coordinates of Stations Used in the Study

Name	Geo Lat	Geo Long	Instrument	Model
Cambridge Bay (CBB)	69.101929 N	254.884829 E	GISTM/GPS	GSV4004B
Eureka (EUR)	79.990089 N	274.097557 E	GISTM/GPS	GSV4004B
Rabbit Lake (RAB)	58.226935 N	256.322945 E	GISTM/GPS	PolaRxS

In this paper, we are researching subtly the overall effect of the St. Patrick's Day tempests of March 2015 on the ionosphere over the northern polar cap locale. Exceptionally compelling are the positive ionospheric storms saw at the northern polar stations Cambridge Bay, Eureka and Rabbit Lake in the attractive tempests, which propose that the plasma thickness develops along these lines during comparable geophysical conditions. While the commitments of different tempest time wonders toward the arrangement of TOI during these tempests have been broadly contemplated, the job of outer driving instruments in altering the reaction of the polar ionosphere has not been focused. Consequently, the principle objective of the investigation is to break down exhaustively the systems that lead to the age of positive ionospheric storms over the northern polar cap area. In the accompanying, we depict our outcomes in subtleties and talk about their importance in creating comprehension of the reaction of the Earth's polar ionospheric framework to geomagnetic storms.

Result

Observation of geomagnetic condition we are describing in figure 2. The severe geomagnetic storm occurred on 17 March 2015 and caused the dramatic response in the ionosphere–plasmasphere–magnetosphere system. Figure 1 shows the variations of interplanetary and geomagnetic parameters during 15–20 March 2015.

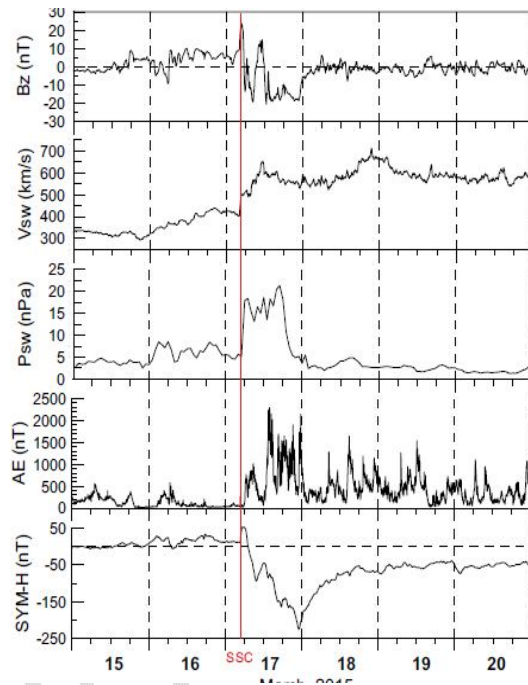


Fig 2. Observation of geomagnetic condition

The sudden storm commencement (SSC) was registered at ~0445 UT and then there was a quick drop of the SYM-H index to the value of -226 nT, observed at ~2300 UT, with a couple of local minima of -93 and -164 nT at ~0940 and ~1740 UT respectively (Fig. 1). The planetary index of the geomagnetic activity K_p reached the maximum value of 8 after ~12 UT on 17 March 2015, qualifying it as a severe geomagnetic storm. During the main phase of the storm (17 March), the interplanetary magnetic field (IMF) orientation displayed a highly complex behavior. Three IMF components (top panels of Fig. 1) switched several times from positive to negative values and vice versa. Right after the shock arrival, the northward IMF B_z component reached the value of about 25 nT. At ~0530 UT the IMF B_z turned southward and reached the first minimal value of -18 nT at 0615 UT. Then the IMF B_z sharply turned northward and varied significantly between north and south during ~8 h. After ~1340 UT the B_z turned southward again and remained south till the end of this day. From ~06 till 11 UT, there are observed

dominating positive B_x and negative B_y with peak values of 16.5 and -16.8 nT for B_x and B_y , respectively. During 11–15 UT with the new southward turning of B_z , the opposite situation with B_x/B_y domination occurred— B_x became negative with the minimal values of -14 nT while B_y component became positive with the peak of 30 nT. After 15 UT, IMF B_y turned sharply to negative values, reaching -8 nT, and then again to the positive ones with the new peak of 20 nT around 18 UT. Kamide and Kusano (2015) reported that this severe geomagnetic storm (G4 level) was a result from the superposition of two successive, moderate storms, driven by two successive, southward IMF structures. The intense geomagnetic storm on 17–18 March 2015 leads to the auroral particle precipitation and an enhancement of the substorm activity.

Response of the High latitude northern ionosphere

To understand the plasma density variations in the southern polar ionosphere during 17 March 2015, we examined the variation of TEC at the Arctic stations, is shown in Figures 3 respectively

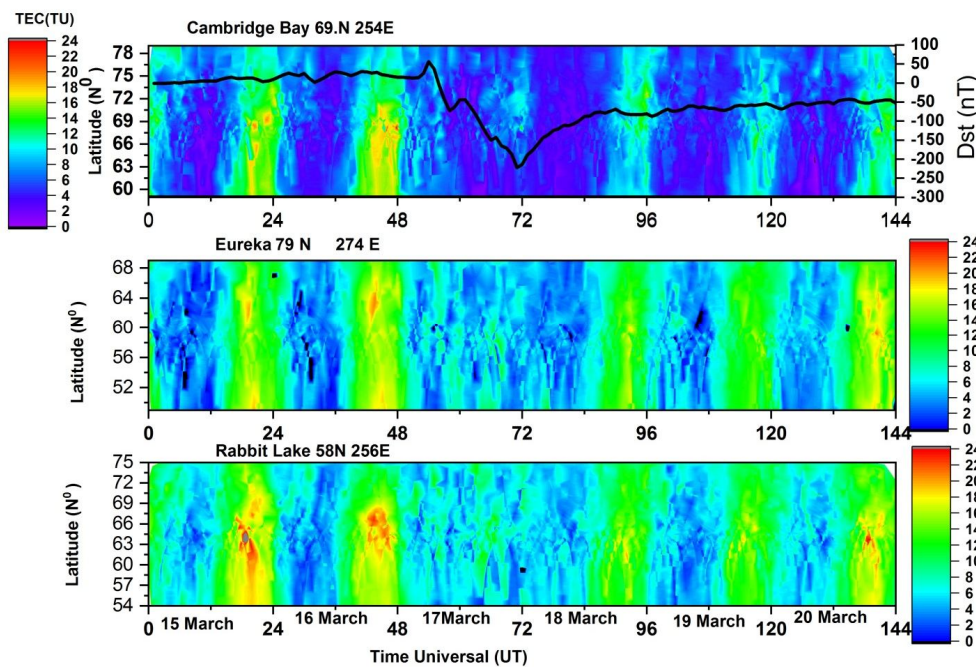


Figure 3. TEC variation over Arctic Region ionosphere during 15-20, March 2015

Figure 3 is composed of four panel including Dst fluctuation during storm from 15 march to 20 march over arctic region. TEC data are plotted with time and latitude scale during the storm period, from the first panel showing the TEC fluctuation over Cambridge Bay, during the observation we notice the TEC is decreasing (<8 TECU) during the storm time and after 24 hrs

it's taking regular pattern, whole period of storm there is very less TEC observed. Second panel of figure showing Eureka station, there is also TEC activity is decreasing(>10 TECU) but little bit high as compare with Cambridge way we can see clearly in graph. Panel third is showing Rabbit Lake, there is TEC activity is high(>12 TECU) as compare to both stations.

Discussion

Above segment we depicted exhaustively the perceptions. In this part, we will examine point by point the outcomes all together toward decipher them. In Table 2, we have set up together the fundamental attributes of the tempest relying upon the longitudinal. There are a few actual systems for the arrangement of ionospheric anomalies in the polar ionosphere during TOI advancement, specifically Kelvin–Helmholtz and slope float instabilities (e.g., van der Meeren et al. 2014). Sojka et al. (1998) examined one such component. For the March 17, 2015 tempest, the two elements of the quick unbiased and plasma streams, affirmed by the Millstone Hill ISR estimations along with outdoors plasma upgrade (got from Swarm LP and outdoors GPS TEC estimations), support that ideal conditions for GDI advancement caused the event of the plasma thickness inconsistencies in the outdoors ionosphere. Expanded amplitudes of TEC varieties with expanding coupling rate probably mirror an expanded power of vivacious molecule precipitation, expanded thickness of polar patches comparative with the ionospheric foundation thickness, and, as a rule, a more unique and tempestuous polar cap with expanded magnetospheric convergence of sun oriented breeze energy. Biggest sufficiency TEC varieties were seen across early afternoon at scopes of 74.0–78.0° MLat. Huge post-noon amplitudes were noticed for lower coupling rates (<5000) and keeping in mind that prenoon and early afternoon amplitudes were biggest for higher coupling rates (>5000). These appropriations demonstrate expanded precipitation power in the post-noon area with expanded coupling rate and extraordinary precipitation around early afternoon and prenoon for high coupling rates >5000. Nilsson et al. [1998] noticed E district ionization because of particle precipitation at areas planning to the low scope cusp, in spite of the fact that it is hazy whether expanded coupling rates would strengthen this precipitation. The attractive field that interfaces the high-latitude ionosphere to the magnetosphere permits the immediate passage of particles of sunlight based breeze and magnetospheric beginning into the polar ionosphere during calm/upset occasions. The power of these cycles improves during times of toward the south interplanetary attractive field (IMF) which is an important condition for the magnetopause disintegration (Aubry et al., 1970; Meng, 1970). Dayside reconnection brings about the reallocation of attractive motion and fortifying of the magnetospheric convection electric fields and field-aligned flows, prompting polar cap development and equatorward development of the auroral oval (Le et al., 2016). The high-latitude ionosphere is likewise influenced by the attractive substorms (Elphinstone et al., 1996).

Comment [APBS3]: Split this paragraph into three or four according to your results

CONCLUSION

When compared to previous tempests, March 17, 2015 was much larger in area and moved in accordance with the strength of the geomagnetic storm. The 2015 St. Patrick's Day storm was a particularly turbulent time, with strong coupling of the SWMI framework throughout the storm's principal phase. Better plasma thickness was seen in the TOI formed in the southern polar cap on March 17, 2015. This is due to the astounding coupling of the sunlight-based wind-magnetosphere-ionosphere framework over extended distances via electric fields and nonpartisan winds. Since the early principal era of the tempest, more grounded storm time electric fields have been prevalent due to the solid and supported magnetopause disintegration on March 17, 2015. This analysis demonstrates that the high-magnitude plasma thickness dissemination's spatiotemporal development is significantly influenced by the length and degree of magnetopause disintegration.

This study illustrates how the behavior of the polar ionosphere is directly influenced by external geomagnetic storm drivers and provides insight into the concept of the sun-facing wind's relationship to the earth's IT system on St. Patrick's Day, 2015. This article uses GPS perceptions to investigate ionospheric responses to the geomagnetic storms on March 17, 2015. We summarize our main findings as follows:

During the storm period of March 15–20, 2015, across the arctic region, total electron content fluctuation was quite low and took a consistent pattern after 24 hours. In addition, there is TEC activity over Eureka station, which is slightly higher than over Cambridge Way but still declining. When compared to the other two stations, the Rabbit Lake station experiences higher TEC activity during the storm.

Reference

- van der Meeren C, Oksavik K, Lorentzen D, Moen JI, Romano V (2014) GPS scintillation and irregularities at the front of an ionization tongue in the nightside polar ionosphere. *J Geophys Res Space Phys* 119:8624–8636. doi:10.1002/2014JA020114
- Aubry, M. P., Russel, C. T., & Kivelson, M. G. (1970). Inward motion of the magnetopause before a substorm. *Journal of Geophysical Research*, 75, 7018–7031. <https://doi.org/10.1029/JA075i034p07018>.
- Buonsanto, M. J. (1999). Ionospheric storms-Review. *Space Science Reviews*, 88, 563–601.
- Elphinstone, R. D., Murphree, J. S., & Cogger, L. L. (1996). What is a global auroral substorm? *Reviews of Geophysics*, 34, 169–232.
- Gonzalez, W. D., Joselyn, J. A., Kamide, Y., Kroehl, H. W., Rostoker, G., Tsurutani, B. T., & Vasyliunas, V. M. (1994). What is a geomagnetic storm. *Journal of Geophysical Research*, 99(A4), 5771–5792.

Le, G., Luhr, H., Anderson, B. J., Strangeway, R. J., Russell, C. T., Singer, H., et al. (2016). Magnetopause erosion during the 17 March 2015 magnetic storm: Combined field-aligned currents, auroral oval, and magnetopause observations. *Geophysical Research Letters*, 43, 2396–2404. <https://doi.org/10.1002/2016GL068257>.

Meng, C. I. (1970). Variation of the magnetopause position with substorm activity. *Journal of Geophysical Research*, 75, 3252.

Prölss, G. W. (1995). Ionospheric F-region storms. In H. Volland (Ed.), *Handbook of atmospheric electrodynamics* (Vol. 2, pp. 195–248).

Mendillo, M., 2006. Storms in the ionosphere: patterns and processes for total electron content. *Rev. Geophys.* 44, RG4001. <https://doi.org/10.1029/2005RG000193>.

Fuller-Rowell, T.J., Codrescu, M.V., Rishbeth, H., Moffett, R.J., Quegan, S., 1996. On the seasonal response of the thermosphere and ionosphere to geomagnetic storms. *J. Geophys. Res.* 101, 2343–2353.

Bilitza, D., and B. W. Reinisch (2008), International Reference Ionosphere 2007: Improvements and new parameters, *Adv. Space Res.*, 42, 599–609, doi:10.1016/j.asr.2007.07.048.

Jayachandran, P. T., et al. (2009), Canadian High Arctic Ionospheric Network (CHAIN), *Radio Sci.*, 44, RS0A03, doi:10.1029/2008RS004046.

Jayachandran, P. T., C. Watson, I. J. Rae, J. W. MacDougall, D. W. Danskin, R. Chadwick, T. D. Kelly, P. Prikryl, K. Meziane, and K. Shiokawa (2011), High-latitude GPS TEC changes associated with a sudden magnetospheric compression, *Geophys. Res. Lett.*, 38, L23104, doi:10.1029/2011GL050041.

Jayachandran, P. T., K. Hosokawa, K. Shiokawa, Y. Otsuka, C. Watson, S. C. Mushini, J. W. MacDougall, P. Prikryl, R. Chadwick, and T. D. Kelly (2012), GPS total electron content variations associated with poleward moving Sun-aligned arcs, *J. Geophys. Res.*, 117, A05310, doi:10.1029/2011JA017423.

Nilsson, H., S. Kirkwood, and T. Moretto (1998), Incoherent scatter radar observations of the cusp acceleration region and cusp field-aligned currents, *J. Geophys. Res.*, 103, 26,721–26,730, doi:10.1029/98JA02269.

Prikryl, P., P. T. Jayachandran, R. Chadwick, and T. D. Kelly (2015), Climatology of GPS phase scintillation at northern high latitudes for the period from 2008 to 2013, *Ann. Geophys.*, 33, 531–545, doi:10.5194/angeo-33-531-2015.

Burns, A. G., T. L. Killeen, W. Deng, G. R. Carignan, and R. G. Roble (1995), Geomagnetic storm effects in the low-latitude to middle-latitude upper thermosphere, *J. Geophys. Res.*, 100, 14,673–14,691, doi:10.1029/94JA03232.

Richmond, A. D., and G. Lu (2000), Upper-atmospheric effects of magnetic storms: A brief tutorial, *J. Atmos. Sol. Terr. Phys.*, 62, 1115–1127, doi:10.1016/S1364-6826(00)00094-8.

Prölss, G. W. (1995), Ionospheric F-region storms, in *Handbook of Atmospheric Electrodynamics*, edited by H. Volland, pp. 195–248, CRC Press, Boca Raton, Fla.

UNDER PEER REVIEW